

# Current Control Strategy for Brushless DC Motors Based on a Common DC Signal

Juan W. Dixon and Iván A. Leal

**Abstract**—A simplified current controlled modulation technique for brushless dc motors is presented. It is based on the generation of quasisquare-wave currents, using only one current controller for the three phases. The advantages of this strategy are

- a) very simple control scheme;
- b) the phase currents are kept balanced;
- c) the difficult sensing of dc link current in flat plates is avoided;
- d) the current is controlled through only one dc component.

These characteristics allow to use the triangular carrier as a current control strategy for the power transistors, which is simpler and better than other options. Computer simulations using power electronic simulator (PSIM), have been developed to show the good characteristics of this solution, and its simplicity. Some experiments with a 15 kW motor-inverter system, show the excellent behavior under steady-state, and transient situations, such as step response and reversal of power.

**Index Terms**—Motor-inverter system, power transistors, PSIM.

## I. INTRODUCTION

**I**N ELECTRIC traction, like in other applications, a wide range in speed and torque control for the electric motor is desired. The dc machine fulfils these requirements, but this machine needs periodic maintenance. The ac machines, like induction motors, and brushless permanent magnet motors do not have brushes, and their rotors are robust because commutator and/or rings do not exist. That means very low maintenance. This also increases the power-to-weight ratio and the efficiency. For induction motors, flux control has been developed, which offers a high dynamic performance for electric traction applications [1], [2]. However, this control type is complex and sophisticated. The development of brushless permanent magnet machines [3]–[5] has permitted an important simplification in the hardware for electric traction control. Today, two kinds of brushless permanent magnet machines for traction applications are the most popular:

- 1) permanent magnet synchronous motor (PMSM), which is fed with sinusoidal currents
- 2) brushless dc motor (BDCM), which is fed with quasisquare-wave currents.

These two designs eliminate the rotor copper losses, giving very high peak efficiency compared with a traditional induction

motor (around 95% in Nd–Fe–B machines in the range 20 to 100 kW). Besides, the power-to-weight ratio of PMSM and BDCM is higher than equivalent squirrel cage induction machines. The aforementioned characteristics, and a high reliability control make this type of machine a powerful traction system for electric vehicle applications [6].

The research introduced in this paper is guided to give a simple and efficient modulation control system, which allows to have good current waveforms. In order to fulfil these objectives, a BDCM was used because of the following advantages:

- 1) the quasisquare-wave armature currents are mainly characterized through their maximum amplitude values, which directly controls the machine torque;
- 2) the position sensor system for the shaft needs only to deliver six digital signals for commanding the transistors of the inverter;
- 3) the inverter performance is very much reliable, because there are natural dead times for each transistor.

The first characteristic allows to design a circuit for controlling only a dc component, which represents the maximum amplitude value of the trapezoidal currents,  $I_{MAX}$ . The second and third characteristics allow to reduce the complex circuitry required by other machines, and allows the self-synchronization process for the operation of the machine.

The most popular way to control BDCM for traction applications is through voltage-source current-controlled inverters. The inverter must supply a quasisquare current waveform whose magnitude,  $I_{MAX}$ , is proportional to the machine shaft torque [7]. Then, by controlling the phase-currents, torque and speed can be adjusted. There are two ways to control the phase-currents of a BDCM:

- 1) through the measurement of the phase currents, which are compared and forced to follow a quasisquare template;
- 2) through the measurement of the dc link current, which is used to get the magnitude of the phase-currents,  $I_{MAX}$ .

In the first case, the control is complicated, because it is required to generate three, quasisquare current templates, shifted  $120^\circ$  for the three phases. Besides, these current templates are not easy to follow for the machine currents, because of phase-shifts and delays introduced [8]. In the second case, it is difficult to measure the dc current, because the connection between transistors and the dc capacitors in power inverters are made with flat plates to reduce leakage inductance. Then, it becomes difficult to connect a current sensor. To avoid those drawbacks, in this paper the equivalent dc current is obtained through the sensing of the armature currents. These currents are rectified, and a dc component, which correspond to the amplitude  $I_{MAX}$

Manuscript received July 26, 2000; revised December 7, 2001. This work was supported by Conicyt through Fondecyt Project 1990097. Recommended by Associate Editor G. K. Dubey.

The authors are with the Department of Electrical Engineering, Pontificia Universidad Católica de Chile, Santiago 6904411, Chile (e-mail: jdixon@ing.puc.cl).

Publisher Item Identifier S 0885-8993(02)02249-4.

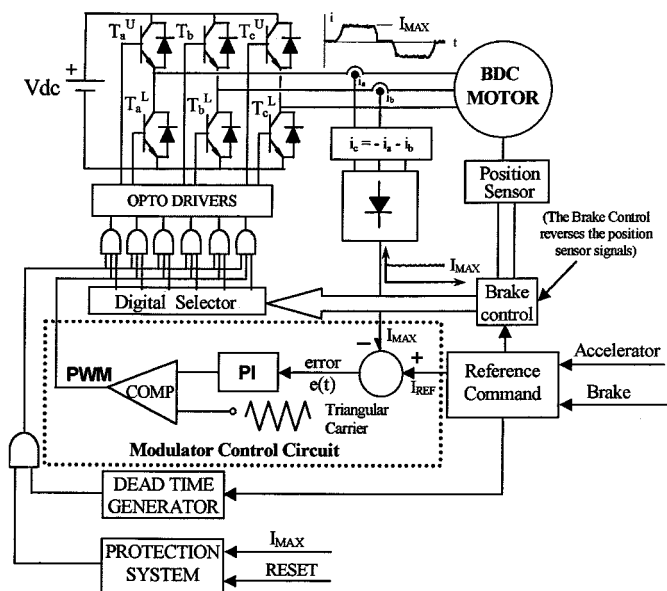


Fig. 1. Proposed control strategy for BDCM.

of the original phase currents is obtained. This dc component is then used to drive the BDCM. The advantages of this strategy are:

- a) the stator currents are completely characterized by their maximum amplitude;
- b) the three phases are controlled with the same dc component, and then the phase currents are kept at exactly the same magnitude  $I_{MAX}$ ;
- c) the dc link current measurement is not required.

These characteristics allow to use the triangular carrier as a current control strategy for the power transistors, which is simpler and more accurate than other modulation methods [8].

## II. PROPOSED CONTROL SYSTEM

Fig. 1 shows a schematic of the proposed control strategy. The operation of the system is as follows: as the motor is of the brushless dc type, the waveforms of the armature currents are quasisquare. These currents are sensed through current sensors, and converted to voltage signals. These signals are then rectified, and a dc component, with the value of the ceiling of the currents,  $I_{MAX}$ , is obtained as shown in Fig. 1. This dc signal  $I_{MAX}$  is compared with a desired reference  $I_{REF}$ , and from this comparison, an error signal “ $e(t)$ ” is obtained. This error is then passed through a PI control to generate the PWM for all the six valves of the inverter, which are sequentially activated by the shaft position sensor. The torque is directly commanded by  $I_{REF}$ . The larger the reference  $I_{REF}$ , the higher the torque produced. The strategy becomes simple, because the control only needs to be in command of one dc current instead of three alternating waveforms. Another advantage of this strategy is that the modulation of the currents can be done using one of the simplest control strategy available: the “triangular carrier modulation strategy” which offers the following additional advantages:

- 1) the switching frequency becomes defined by the triangular carrier

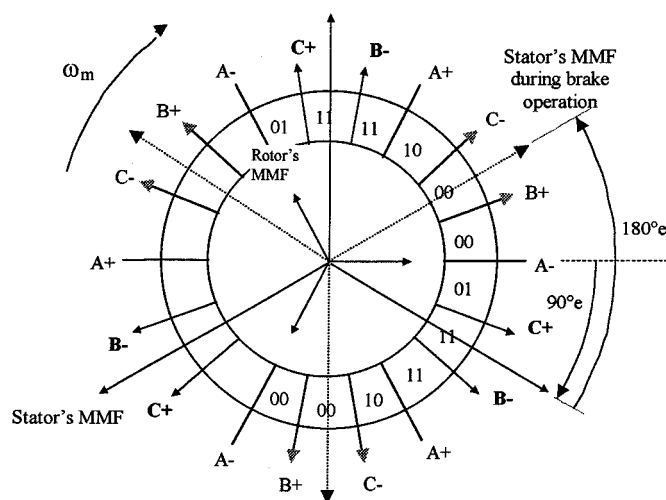


Fig. 2. Stator and rotor’s MMF during step change from motor to brake operation.

- 2) the ability to follow the template with the proposed method becomes quite accurate when triangular carrier is used
- 3) the hardware implementation is very simple.

The control strategy also allows regenerative braking, which is very important in many applications, like electric vehicles, where energy can be returned to the battery pack. To brake the motor (regenerative braking) the stator magnetic field is reversed. This action is accomplished through the inversion of the signals given by the position sensor. The Fig. 2 shows graphically the rotor and stator magnetic fields for a six-pole machine (three pair of poles). The position sensor discriminates six positions each 360 electric degrees. During motor operation, the rotor moves clockwise. When the brake signal is applied, the stator field is reversed 180 electric degrees. This action produces an instantaneous change in the direction of the torque, making a fast reduction of the speed of the machine, which begins to return its energy to the dc link. The same strategy can be used for reversal of rotation of the machine.

## III. CIRCUIT DESIGN

The drive system consist of a three-phase 20 [kW] inverter, a 16 [HP] BDC permanent magnet motor, and a dc power supply. The sensing system is divided in two parts: *Position Sensor System* and *Current Sensor System*. The first system is based on three hall effect cells placed inside the motor, and a magnetic disc in the rotor, with the same number of poles as the motor. The second sensing system (armature current) is based on two LEM modules placed in any of the three phases of the motor. The measurement of the currents in the three phases is not required because of the following:

- a) there is no neutral connection, and hence the third phase-current can be obtained from the other two;
- b) despite the first reason is more than enough to justify the use of only two current sensors, there is another reason which could justify just one current sensor: the sensing of the current is only required to get the value of the mag-

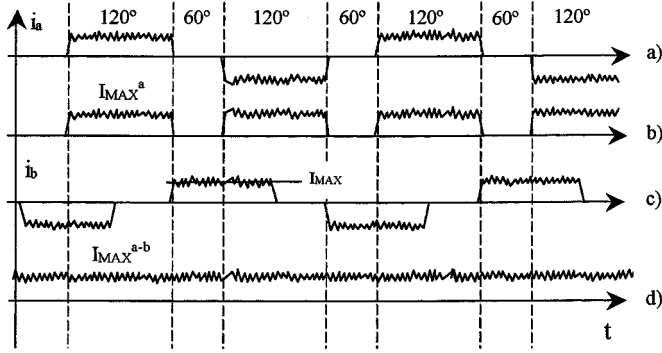


Fig. 3. Generation of  $I_{MAX}$  through the phase currents: (a) phase-a current, (b) rectified current signal using only one phase, with  $120^\circ$  missing information, (c) phase-b current, and (d) rectified current signal using two phases, with complete information of  $I_{MAX}$ .

nitude  $I_{MAX}$  (the phase-shift and sequence is given by the position sensor).

Assuming only one current sensor, it could be possible to get information of the current  $I_{MAX}$  during  $2/3$  of the cycle ( $240^\circ$ ). For the other  $120^\circ$ , the PWM could be maintained with the same duty cycle until the next information of  $I_{MAX}$  is obtained. The one-sensor system could work well under normal balanced conditions in motor windings and inverter characteristics, and with slow dynamic operation. However, in general conditions is safer and more accurate to have at list two current sensors, which already give redundant information. The Fig. 3 shows graphically the way  $I_{MAX}$  is obtained through one phase-current sensor, and through two current sensors. Clearly, the information of one current sensor could be used, providing that the PWM is kept with constant duty cycle during the two intervals of  $60^\circ$  were no information about  $I_{MAX}$  is obtained. However, the information with two sensors is complete and redundant as shown in the same Fig. 3.

As it was already mentioned, the utilization of one current sensor at the dc link is not possible, because the power inverter was implemented using flat cooper plates between transistors and electrolytic capacitors. This is the common way to construct power inverters, because otherwise the leakage inductance between dc link and transistors becomes very large, producing dangerous over voltages that could destroy the power transistors.

The **Modulator Control Circuit** of the Fig. 1 has subblocks of analog and digital electronic circuits (comparators, PI controller, and adder devices). As it was already mentioned, the dc signal  $I_{MAX}$  is obtained from signal rectification of the phase-currents. This rectification system uses germanium diodes to reduce the nonlinearity problem introduced by the fixed voltage drop of the diodes used in the rectifier. However, this problem becomes noticeable only when the current is smaller than 3% of the nominal value of  $I_{MAX}$  (120 A). Then, it does not becomes a serious problem in the operation of the proposed method.

The current  $I_{MAX}$  is compared with a desired reference  $I_{ref}$ , and from this comparison, and error signal " $e(t)$ " is obtained. This error signal  $e(t)$  is then processed with a PI control. The

output of the PI control is compared with a triangular waveform of fixed amplitude and frequency, which gives a common and unique pulse width modulation for the three phases of the motor. This unique PWM pattern, and the information given by the position sensor, generates the modulation signals for each transistor. The PWM controls the magnitude  $I_{MAX}$ , and the position sensor discriminates when the PWM has to be applied to each of the six transistors, creating the correct sequence for the rotation of the machine. The Fig. 4 shows the digital operation of the position sensor.

#### IV. CURRENT CONTROLLER DESIGN

The tuning of the current controller starts with the determination of the amplitude and frequency of the triangular carrier, and the gains of the PI control. To get a PWM signal operating at the carrier frequency, the control should be adjusted to keep the reference current moving around the reference. The Fig. 5 shows the way the stator currents are controlled, through the feedback signal  $I_{MAX}(t)$ . The slopes  $m_1$  (up) and  $m_2$  (down) are a function of the dc link voltage, and the motor model. The motor model comprises the phase inductance, and the back emf [9]. Then, the maximum error based on a carrier  $e_{MAX}$  will depend on the slopes  $m_1$  and  $m_2$ , and hence on the operating point, and the carrier frequency. This situation can be expressed mathematically, with the help of Fig. 5, as seen in

$$\left. \begin{aligned} |m_1| &= \frac{E_{PP}}{xT} = \frac{E_{PP} \cdot f}{x} \\ |m_2| &= \frac{E_{PP}}{(1-x)T} = \frac{E_{PP} \cdot f}{1-x} \end{aligned} \right\} \rightarrow E_{PP} = \frac{1}{f} \cdot \frac{|m_1| \cdot |m_2|}{|m_1| + |m_2|} \quad (1)$$

The term " $x$ " in (1) represents the fraction of the period of the carrier, " $T$ ," when the current is increasing. According with this equation, the term " $x$ " defines the ideal output of the PWM pattern. Then, the control parameters have to be adjusted according with the index " $x$ ." Note that  $E_{PP}$  represents the "peak-to-peak" error of the signal.

According to the time reference of Fig. 5, the following relations can be written:

$$\left. \begin{aligned} (t_2 + t_1) &< x \cdot T \\ (t_2 - t_1) &= x \cdot T \\ |t_2| &\leq |t_1| \\ e(t_2) + e(t_1) &= 0 \\ e(t_2) - e(t_1) &= E_{PP} \\ e(t_1) &= \frac{E_{PP}}{2} \end{aligned} \right\} \quad (2)$$

Now, when the current  $I_{MAX}$  is increasing, the error  $e(t)$  can be modeled as

$$e(t) = -m_1 \cdot t + n_1, \quad \text{para } t \in [t_1, t_2]. \quad (3)$$

If the rate of conversion of the magnitudes is  $1 : \alpha$ , then the expressions of the error  $e_{ci}(t)$  becomes as shown in

$$e_C(t) = \alpha \cdot e(t). \quad (4)$$

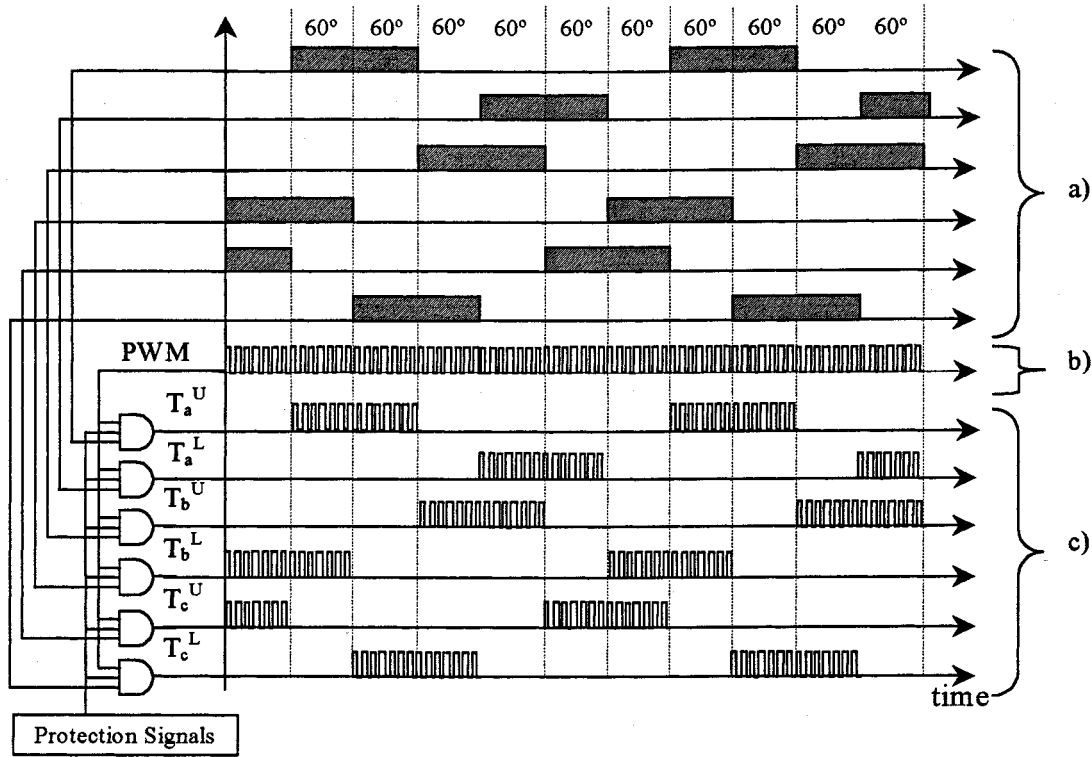


Fig. 4. Digital operation of the position sensor: (a) position sensor signals, (b) PWM signal, and (c) gating signals for the IGBTs.

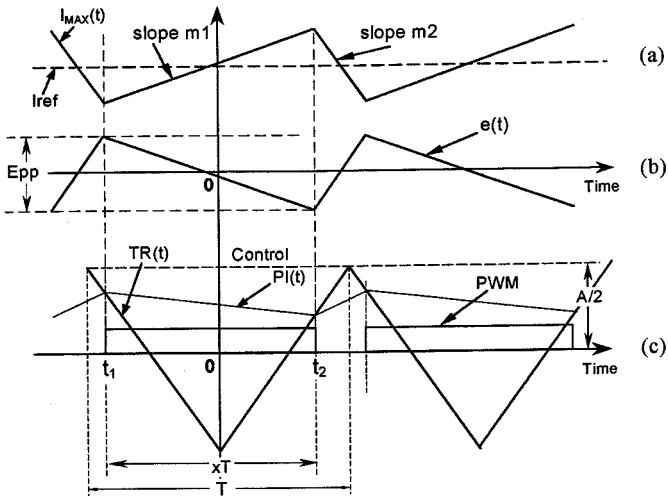


Fig. 5. Ideal waveforms of (a) feedback signal  $I_{MAX}$ , (b) error signal  $e(t)$ , and (c) control signals.

On the other hand, the output of the PI control can be expressed as:

$$PI(t) = K_P \cdot e_C(t) + K_I \cdot \int_0^{t_1} e_C(t) \cdot dt \quad (5)$$

Now, if we assume that the operation of the machine is stable, and operates under steady-state, the integrator output is close to a constant. That means

$$M = K_I \cdot \int_0^{t_1} e_C(t) \cdot dt = \text{constant}. \quad (6)$$

The triangular carrier and the PI output have the same value at  $t_1$  and  $t_2$ , because these are intersections points that define the PWM generation

$$PI(t_1) = TR(t_1) \Rightarrow K_P \cdot e_C(t_1) + M = -\frac{2 \cdot A}{T} \cdot t_1 - \frac{A}{2} \quad (7)$$

$$PI(t_2) = TR(t_2) \Rightarrow K_P \cdot e_C(t_2) + M = \frac{2 \cdot A}{T} \cdot t_2 - \frac{A}{2}. \quad (8)$$

With (7) and (8),  $K_P$  and  $M$  are obtained

$$K_P = \frac{\frac{2 \cdot A}{T} \cdot (t_2 + t_1)}{\alpha \cdot (e(t_2) - e(t_1))} < \frac{\frac{2 \cdot A}{T} \cdot x \cdot T}{\alpha \cdot (e(t_1) - e(t_2))} \quad (9)$$

$$M = \frac{1}{2} \left[ \frac{2A}{T} (t_2 - t_1) - A - K_P \cdot \alpha \cdot (e(t_2) + e(t_1)) \right]. \quad (10)$$

Now, with the help of (2), (9), and (10), can be resumed as

$$K_P < \frac{1}{\alpha} \cdot \left( \frac{2 \cdot A}{E_{FP}} \right) \cdot x \quad (11)$$

$$M = A \cdot \left( x - \frac{1}{2} \right). \quad (12)$$

Replacing (12) in (6), the value of  $K_I$  is obtained

$$K_I = \frac{A \cdot \left( x - \frac{1}{2} \right)}{\int_0^{t_1} e_C(t) dt} = \frac{A \cdot \left( x - \frac{1}{2} \right)}{\alpha \cdot \int_0^{t_1} e(t) dt}. \quad (13)$$

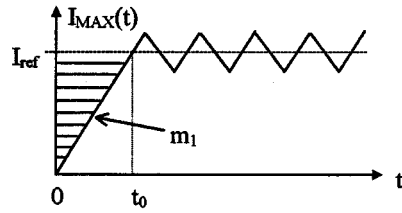


Fig. 6. Approach for the error's integral value.

### A. First Design Condition

The PWM based on the triangular carrier method has to set a commutation frequency lower than (or equal to) the carrier. This condition can be expressed as

$$2Af \geq \frac{dPI_2(t)}{dt} \Rightarrow 2Af \geq K_P \alpha |m_2|. \quad (14)$$

In other words, the slope of the PI control must not exceed the slope of the carrier. The (14) gives a design condition related with the carrier amplitude ( $A$ ) and frequency ( $f$ ), and the proportional gain ( $K_P$ ). On the other hand, an expression related with the integral gain  $K_I$  is not obtained in a straight way.

### B. Second Design Condition

To get  $K_I$ , it has been proposed in [8], as a starting point, to consider the integral gain as the product of the proportional gain with the carrier frequency. However, it is possible to get an approximate expression using (6) and the graphics of Fig. 6, as shown in

$$K_I = \frac{M}{\int_0^t e_c(t) dt} \Rightarrow K_I \leq \frac{2M|m_1|}{\alpha(I_{ref})^2} \quad (\text{approximate expression}). \quad (15)$$

To close the control loop, it is required to estimate the integral error under steady-state conditions. One way to do that is to assume that the value of the integral is higher than the one given by the integration of the error at the initial interval. This is better explained with the help of Fig. 6. Then, using expression (15), and the assumption given by Fig. 6, the calibration of the PI control can be initiated.

## V. SIMULATIONS

As the design conditions depend on the speed of the machine, the control was tuned for a speed of 1000 [rpm]. Besides, the motor was simulated with the following parameters per phase:  $R = 12$  [m $\Omega$ ],  $L = 150$  [uH], and  $|e_g|_{MAX} = 20$  [V/krpm]. The power inverter was assumed ideal, and the dc link supply was set at 144 [V<sub>dc</sub>]. All these values are in agreement with the real parameters. The next step was to get the value of “ $x$ ” and “ $e_{MAX}$ ”. With these considerations, the values of  $m_1$  and  $m_2$  can be obtained

$$\begin{aligned} m_1 &= \frac{V - 2E}{2L} = \frac{144 - 2 \cdot 20}{2 \cdot 0.000150} = 346\,667 \left[ \frac{A}{s} \right] \\ m_2 &= \frac{-V - 2E}{2L} = \frac{-144 - 2 \cdot 20}{2 \cdot 0.000150} = -613\,333 \left[ \frac{A}{s} \right]. \end{aligned} \quad (16)$$

$$\begin{aligned} \int_0^t e_c dt &\geq \int_0^{t_0} e_c dt \approx \frac{(\alpha I_{ref}) t_0}{2} \\ \therefore \int_0^t e_c dt &\geq \frac{\alpha (I_{ref})^2}{2|m_1|} \end{aligned}$$

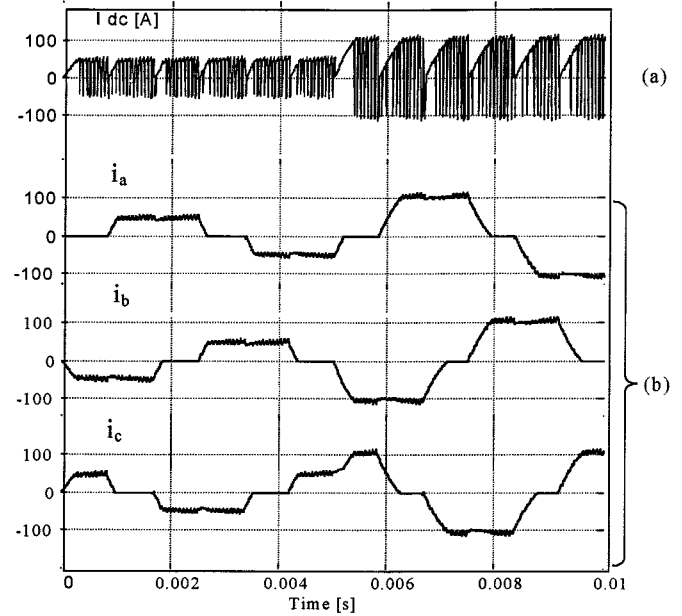


Fig. 7. BDCM armature currents. step change from 50 to 100 [A]: (a) dc link current [A], (b) phase “a” current [A], (c) phase “b” current [A], and (d) phase “c” current [A].

Taking (1), one gets

$$\begin{aligned} x &= \frac{613\,333}{346\,667 + 613\,333} = 0.639 \\ E_{PP} &= \frac{1}{15\,000} \cdot \left( \frac{346\,667 \cdot 613\,333}{346\,667 + 613\,333} \right) = 14.766 \text{ [A]}. \end{aligned} \quad (17)$$

That means at 1000 rpm the PWM has a duty cycle of 63.9%, with a maximum error of  $\pm 7.383$  [A] around the reference. The proportional gain was set in an arbitrary way to a value of 10. This becomes feasible because (14) and (15) are a system with one degree of freedom. On the other hand, the carrier frequency was set at 15 000 Hz (15 kHz). In this form it becomes possible to evaluate the amplitude of the triangular carrier ( $A/2$ ) through (14)

$$A/2 \geq \frac{10 \cdot (1/20) \cdot 613\,333}{4 \cdot 15\,000} = 5.111 \text{ [V]}. \quad (18)$$

Now, the value of the constant “ $M$ ” is obtained through (12), with the results given by (17)

$$M = (0.639 - 1/2)A = 1\,421 \text{ [V]}. \quad (19)$$

Assuming for  $I_{REF}$  a maximum value of 100 [A], and using the results from (16),  $K_I$  can be evaluated

$$K_I \leq \frac{2 \cdot 1.421 \cdot 346.667}{(1/20) \cdot (100)^2} = 1.97. \quad (20)$$

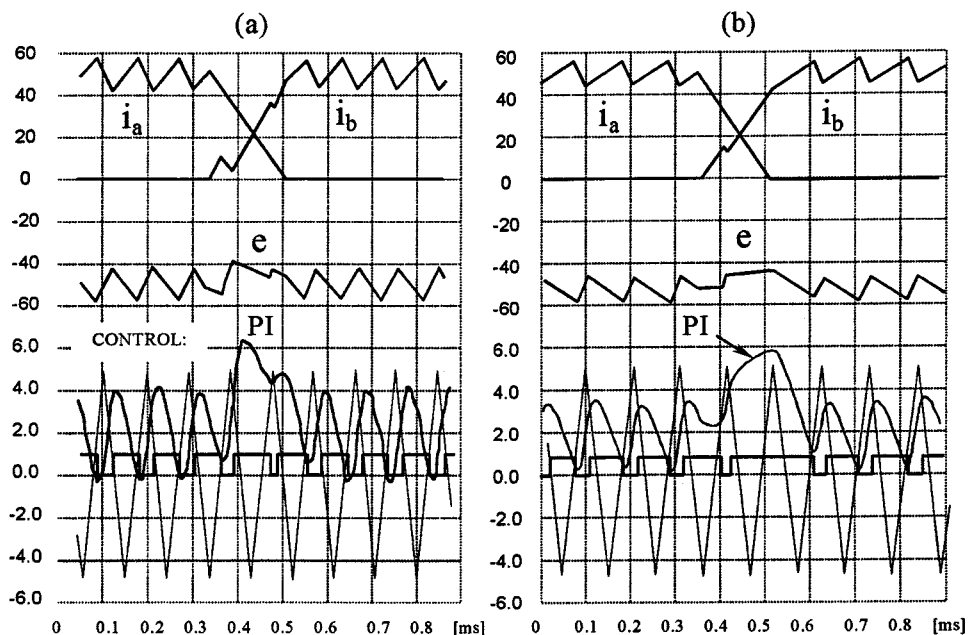


Fig. 8. Modulation details with  $I_{REF} = 50$  [A]: (a) currents per phases and control signals for a 1000 [rpm] operation and (b) currents per phases and control signals for a 2000 [rpm] operation.

To make the simulations, the software power electronics simulator (PSIM) developed by Powersim Technologies Inc., was used. Fig. 7 show the currents per phase of the motor for a step change in the reference current, from 50 to 100 amps in  $I_{MAX}$ . As it can be observed in this figure, the current waveform has a high level of modulation only in their flat zones ( $I_{MAX}$ ). This is because the modulation method used is through  $I_{MAX}$ , and not through a quasi square template.

The simulation of Fig. 8 shows in detail the commutation process between two armature currents (one phase is switched-on and the other is switched-off). The reference current is  $I_{REF} = 50$  [A]. The Fig. 8(a) show armature currents and control signals, for a speed of 1 000 rpm. The same signals, but for a speed of 2 000 rpm are shown in Fig. 8(b). The control signals are from the unique PWM showed in Fig. 1, which resulted from the comparison between the triangular carrier and the PI output. As it can be seen, the PWM controls directly the ON/OFF of the six transistors, which are selected through the phase-commutation given by the position sensor. During the commutation process, the error signal  $e(t)$  becomes larger, but the control keeps the situation under normal conditions once the commutation has finished.

## VI. EXPERIMENTAL RESULTS

Some experiments were performed to evaluate the method of control proposed. The hardware implementation of the experimental work is shown in Fig. 9. The mechanical load was a dc machine. The BDCM is a motor made by Solectria Corporation (Model BRLS 16, 144 [V], 120 [A], six poles, 94% peak efficiency). The IGBT inverter was designed and implemented at our Department of Electrical Engineering (rated values: 150 [V<sub>dc</sub>], 150 [A]). The inverter was fed from a three phase full wave rectifier, and a braking resistor was

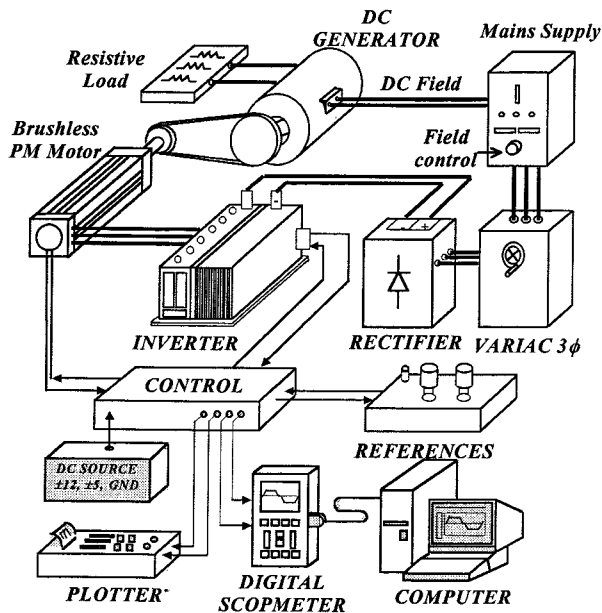


Fig. 9. Diagram of the experimental circuit.

located at the dc link. This braking resistor allowed reversal of power experiments with the BDCM. As can be seen in Fig. 9, phase currents can be plotted and also stored in a personal computer for analysis.

The Fig. 10 shows a current comparison between two methods. Fig. 10(a) shows the current waveform using a quasi-square template and a current controller based on periodical sampling method [8]. On the other hand, Fig. 10(b) shows the current waveforms using the proposed strategy: common PWM pattern for the three phases and current controller based on triangular carrier. The switching frequency has been adjusted to 4 kHz for both the cases. The difference in quality of the

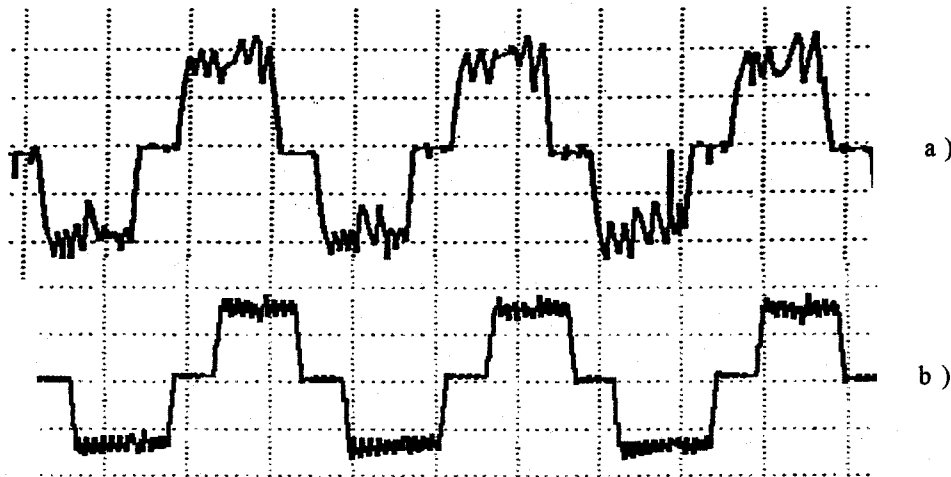


Fig. 10. Armature current waveforms, with  $I_{MAX} = 30$  [A]: (a) conventional method with periodical sampling and quasisquare template and (b) proposed method with triangular carrier and common reference  $I_{REF}$ .

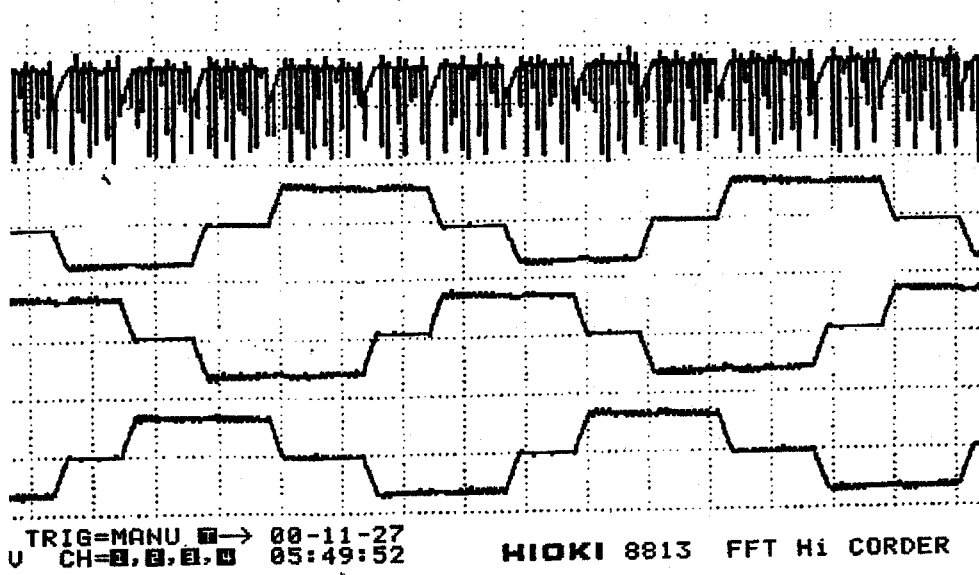


Fig. 11. DC link and phase currents for a 1430 rpm operation (100 A/div).

current waveforms becomes evident. An experiment using common PWM pattern and periodical sampling shows results en between. The same happens when quasisquare template and triangular carrier are used. In one word, the best result is obtained with the proposed method.

The Fig. 11 shows the waveform currents for a reference current  $I_{REF}$  of approximately 80 [A<sub>dc</sub>]. Under the load conditions at the motor shaft, the machine runs at 1430 [rpm]. It can be seen that the phase currents are quite clean. It also can be observed that, because  $I_{MAX}$  is the same for the three phases, the phase currents remain balanced. Currents for other speeds, and reference currents show a similar good performance.

The Fig. 12 shows a step change in the reference current, from  $I_{MAX} = 50$  [A<sub>dc</sub>], to  $I_{MAX} = 100$  [A<sub>dc</sub>]. It can be noted that the change in the current magnitude is clean and without oscillations.

Fig. 13(a) shows a step reversal of power in the reference current, from 50 to  $-80$  amperes in  $I_{MAX}$ . The dc link voltage  $V_{dc} = 120$  v, and the triangular carrier frequency is  $f_c = 15$  kHz. The phase currents  $i_a$  and  $i_b$  are shown. On the other hand, the Fig. 13(b) shows a detail in the transient situation for the current  $i_b$  [see the box in Fig. 13(a)]. The PI control output, the triangular carrier, and the PWM are displayed. It is interesting to see the PI control output, which increases rapidly during the transition, trying to produce the reversal of current as fast as possible.

## VII. CONCLUSION

A different control strategy for brushless dc machines has been presented. It is based on the generation of quasisquare currents using only one current controller for the three phases. The advantages of this strategy are

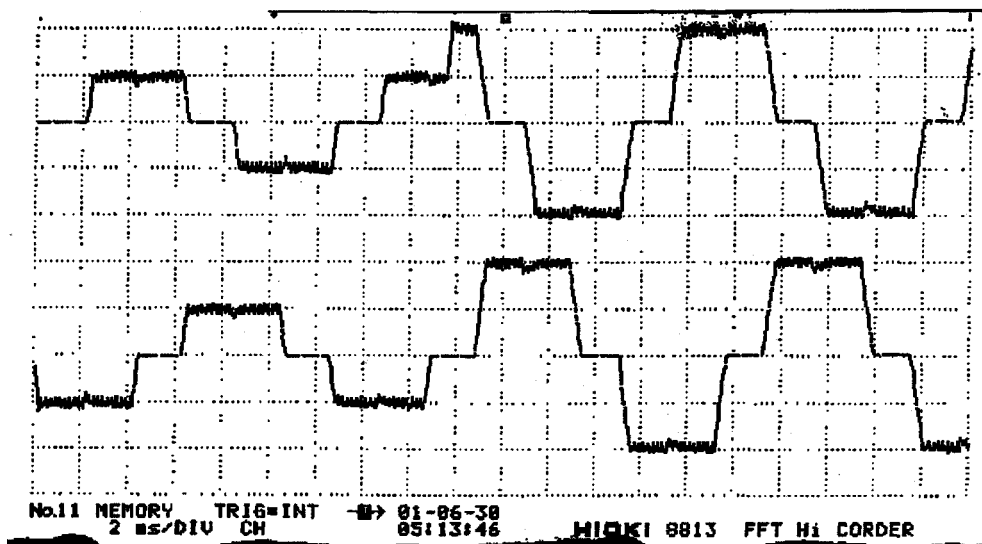


Fig. 12. Step change in  $I_{MAX}$  from 50 to 100 amps.

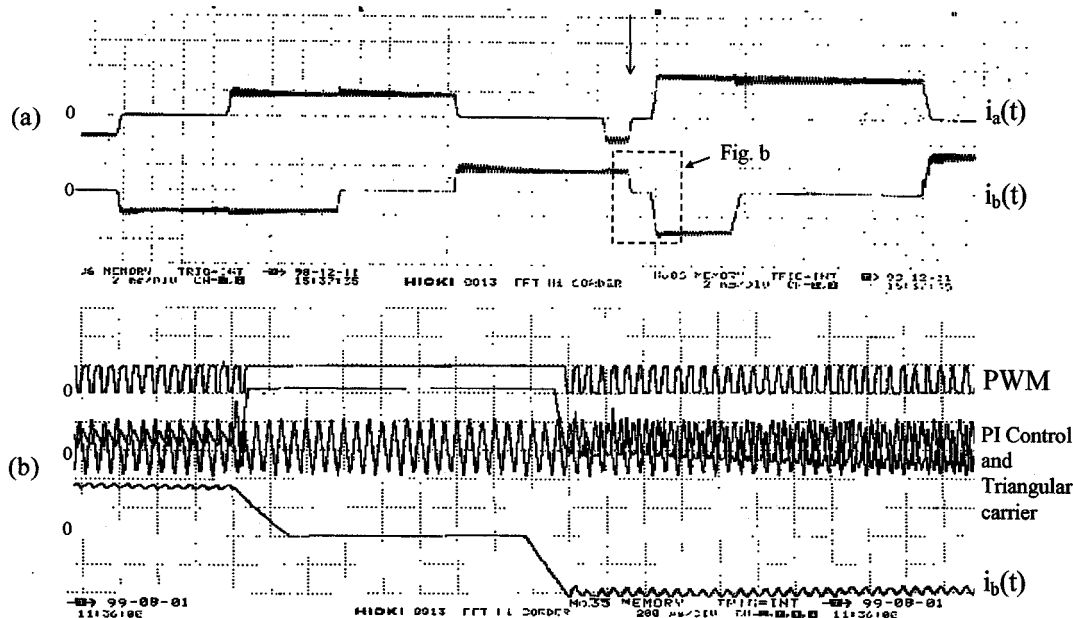


Fig. 13. Reversal of power operation at 400 [rpm], with  $I_{REF}$  from 50 [A] to -80 [A]: (a) line currents and (b) details of signal controls: PWM, triangular carrier, and PI Control output.

- a) very simple control scheme;
- b) phase currents are kept balanced;
- c) current is controlled through a dc component, and hence phase overcurrents are eliminated.

These characteristics allow to use the triangular carrier as a current control strategy for the power transistors, which is simpler and more accurate than other options. This control strategy has been compared with conventional techniques to show the excellent characteristic of this modulation technique. Some experiments with a 15 kW inverter, show the good quality of waveforms under steady-state and transient response. Presently, the work is focused in the use of digital signal processors to implement the method. A DSP controller, based on the TMS 320F241 from Texas Instruments, is being implemented and

programmed, giving good partial results. The idea is to give the system as much flexibility as possible, to investigate the behavior of the system with other options of control, like the one that only needs one phase-current sensor.

REFERENCES

- [1] L. Ben-Brahim and A. Kawamura, "A fully digitised field-oriented controlled induction motor drive using only current sensors," *IEEE Trans. Ind. Electron.*, vol. 39, pp. 241-249, June 1992.
- [2] Y. Xue, X. Xu, T. G. Habetler, and D. M. Divan, "A stator flux-oriented voltage source variable-speed based on dc link measurement," *IEEE Trans. Ind. Applicat.*, vol. 27, pp. 962-969, Sept./Oct. 1991.
- [3] A. R. Millner, "Multi-hundred horsepower permanent magnet brushless disc motors," in *Proc. IEEE Appl. Power Electron. Conf. (APEC'94)*, Feb. 13-17, 1994, pp. 351-355.

- [4] P. Pillay and R. Krishnan, "Application characteristics of permanent magnet synchronous and brushless dc motors for servo drives," *IEEE Trans. Ind. Applicat.*, vol. 27, pp. 986–996, Sept./Oct. 1991.
- [5] T. Low and M. A. Jabbar, "Permanent-magnet motors for brushless operation," *IEEE Trans. Ind. Applicat.*, vol. 26, pp. 124–129, Jan./Feb. 1990.
- [6] C. C. Chan and K. T. Chau, "An overview of power electronics in electric vehicles," *IEEE Trans. Ind. Electron.*, vol. 44, pp. 3–13, Feb. 1997.
- [7] J. M. D. Murphy and F. G. Turnbull, *Power Electronic Control of AC Motors*. Exeter, U.K.: Wheaton & Co., Ltd., 1988, pp. 424–428.
- [8] J. Dixon, S. Tepper, and L. Morán, "Practical evaluation of different modulation techniques for current-controlled voltage source inverters," *Proc. Inst. Elect. Eng.*, vol. 143, pp. 301–306, July 1996.
- [9] N. Hemati and M. C. Leu, "A complete model characterization of brushless dc motors," *IEEE Trans. Ind. Applicat.*, vol. 28, pp. 172–180, Jan./Feb. 1992.



**Juan W. Dixon** (M'90–SM'95) was born in Santiago, Chile. He received the B.S. degree from the University of Chile in 1977 and the M.Eng. and Ph.D. degrees in electrical engineering from McGill University, Montreal, QC, Canada, in 1986 and 1988, respectively.

Since 1979, he has been working at the Catholic University of Chile, where he is an Associate Professor in the Department of Electrical Engineering, in the areas of power electronics and electrical machines. His research interests have included electric traction, machine drives, frequency changers, high power rectifiers, static var compensators, and active power filters.



**Iván A. Leal** was born in Santiago, Chile. He received the B.S. degree in electrical engineering from the Catholic University of Chile in 1999.

Since 1999, he has been working at DMR Consulting, a telecommunications enterprise in Brazil, where he is a Consultor Engineer. His research interests are switching power supplies, power sources for communication equipments, machine drives, and electric traction.